

Tailoring AlGaN nanoalloys with transition metal dopants for enhanced energy storage: A DFT Study

Fatemeh Mollaamin*

Department of Biomedical Engineering, Faculty of Engineering and Architecture, Kastamonu University, Kastamonu, Turkey

*E-mail: fmollaamin@kastamonu.edu.tr

DOI: 10.29303/aca.v8i2.236

Article info:

Received 24/02/2025

Revised 14/03/2025

Accepted 25/06/2025

Available online 29/11/2025

Abstract: The notable fragile signal intensity close to the parallel edge of the nanocluster sample might be owing to silicon or germanium binding induced non-spherical distribution of AlGaSiN or AlGaGeN heteroclusters. However, a considerable deviation exists from doping atoms of palladium or platinum as electron acceptors on the surface of AlGaPdN or AlGaPtN heteroclusters. Then, magnetic parameters exhibited the same tendency of shielding for palladium or platinum; however, a considerable deviation exists from doping atoms of palladium or platinum as electron acceptors on the surface of Pd-AlGaN or Pt-AlGaN hetero-clusters. Therefore, it can be considered that palladium or platinum atoms in the functionalized AlGaPdN or AlGaPtN might have more impressive sensitivity for accepting the electrons in the process of hydrogen adsorption. The advantages of platinum or palladium over aluminum gallium nitride include its higher electron and hole mobility, allowing platinum or palladium doping devices to operate at higher frequencies than silicon or germanium doping devices. As a matter of fact, it can be observed that doped heteroclusters of AlGaPdN or AlGaPtN might ameliorate the capability of AlGaN for energy storage.

Keywords: DFT, metal/metalloid elements; aluminum gallium nitride; H-storage; energy-saving

Citation: Mollaamin, F. (2025). Tailoring AlGaN nanoalloys with transition metal dopants for enhanced energy storage: A DFT Study. Acta Chimica Asiana, 8(2), 768–773. https://doi.org/10.29303/aca.v8i2.245

INTRODUCTION

Group-III-nitride semiconductors have low sensitivity to ionizing radiation which make them appropriate materials for solar cell arrays for satellites. Therefore, space applications could also benefit as devices have shown stability in high radiation environments. Ternary "AlGaN" alloys have been recognized as materials for realizing promising ultraviolet "DUV" optoelectronic devices with operating wavelengths down to 200 nm [1-3]. For the development of high performance AlGaN-based "DUV" devices, high-conductivity p-type Al-rich AlxGa1-xN ($x \ge 0.4$) is essential. Many studies have shown that enhancing the p-type conductivity

has a significant effect on the improvement of both the electrical and optical properties of AIGaN DUV optoelectronics [4–8].

The influence of two different methods of silicon doping in "AlGaN" layer, that is, modulation-doping "MD" and delta-doping "DD", on the optical and electrical performance of deep ultraviolet light-emitting diodes "DUV–LEDs" has been investigated. Both the photoluminescence and electroluminescence intensities in the "Si-DD" structure are stronger than those obtained by the "Si-MD" method, while the forward voltage and reverse leakage current are slightly smaller in the "DD" structure than that in the "MD" structure. Compared with the "MD" structure, the "DD" structure shows higher capacitance-voltage characteristics. This

study suggests that the "DD" method can improve the optical and electrical performance of "DUV-LEDs" [9–11].

In this paper, we propose a feasible ternary semiconductor of aluminum gallium nitride which is doped with silicon, germanium, palladium or platinum. We carried out molecular modelling considering the geometrical parameters of doping atoms on the surface of AlGaN through the absorption status and current charge density of the energy storage was studied.

MATERIALS AND METHODS

Metal/metalloid-doped AlGaN nanocage was calculated within the framework of first-principles calculation based on density functional theory (DFT) (Figure1a-e, a'-e'). The rigid potential energy surface using density functional theory [12-25] was performed due to Gaussian 16 revision C.01 program package [26] and GaussView 6.1 [27]. The coordination input for energy storage has applied 6-311+G (d,p) and EPR-3 basis sets. Development of the applied Density Functional Theory (DFT) methodology only became notable after W. Kohn and L. J. Sham released their reputable series of equations which are introduced as Kohn-Sham (KS) equations [17]. Considering the electronic density within the KS image directs us to a remarkable reduction in quantum computing. Thus, the KS methodology lightens the route for pursuing systems that cannot be conventional discussed by ab-initio methodologies. Kohn and Sham" introduces the solution which brings up the mono-electronic orbitals to account the kinetic energy in a simple and relatively exact, by finding a residual modification that might be computed apart [16].

Therefore, the precise exchange energy functional is described by the Kohn–Sham orbitals in lieu of the density which is cited as the indirect density functional. This research has employed the penetration of the hybrid functional of three-parameter basis set of B3LYP (Becke, Lee, Yang, Parr)" within the conception of DFT upon theoretical computations [18,19].

Theoretical calculations have become essential tools for a comprehensive understanding of the microscopic mechanisms in energy storage materials, particularly in charge density variations and electron transport characteristics behaviors in electrode materials.

In this research article, the calculations have been done by "CAM-B3LYP-D3" level of theory. Dispersion forces were considered under the "DFT-D3" method of Grimme with Becke-Johnson damping. Calculations with spin polarization were performed within the "density functional theory (DFT)" [28]. The exchange correlation potentials were treated using the "Perdew-Burke-Ernzerhof (PBE)" parameterization within the "general gradient approximation (GGA)" [13].

Figure 1 shows the process of energy storage on heteroclusters of AlGaN, AlGaSiN, AlGaGeN, AlGaPdN or AlGaPtN which are varied to maximize the absorption in the active region. Further, we optimized the structural parameters of nanocluster of AlGaN which is doped with silicon, germanium, palladium and platinum towards formation of heteroclusters of AlGaSiN, AlGaGeN, AlGaPdN, and AlGaPtN for obtaining the highest short-circuit current density.

This is a utility used to calculate ring area and perimeter, since ring area is sometimes involved in wavefunction analysis. In this function, it is needed to input the index of the atoms in the ring in clockwise manner including Al5, Si5, Ge5, Pd5, Pt5, N4, Ga15, N7, Ga6, N12 (Figure1a–e, a'–e'). Then, it has be calculated total ring area and total ring perimeter for a tailored ring as 9.6981Å2 and 11.6921 Å2, respectively (Figure1a–e, a'–e').

RESULTS AND DISCUSSION

AlGaPtN for adsorption energy and storage energy.

3.1. NMR and LOL analysis

Based on the resulted amounts, nuclear magnetic resonance (NMR) spectra of Si-AlGaN, Ge-AlGaN, Pd-AlGaN, Pt-AlGaN hetero-clusters as the potential molecules for energy storage can unravel the efficiency of these complexes. From the DFT calculations, it has been attained the chemical shielding (CS) tensors in the principal axes system to estimate the isotropic chemical-shielding (CSI) and anisotropic chemical-shielding (CSA) [29]. The NMR data of isotropic (σ_{iso}) and anisotropic shielding tensors (σ_{aniso}) for ternary alloy of AlGaN and doped hetero-clusters of Si-AlGaN, Ge-AlGaN, Pd-AlGaN, Pt-AlGaN through hydrogen adsorption have been computed by Gaussian 16 revision C.01 program package [26] and been shown in Figure 2.

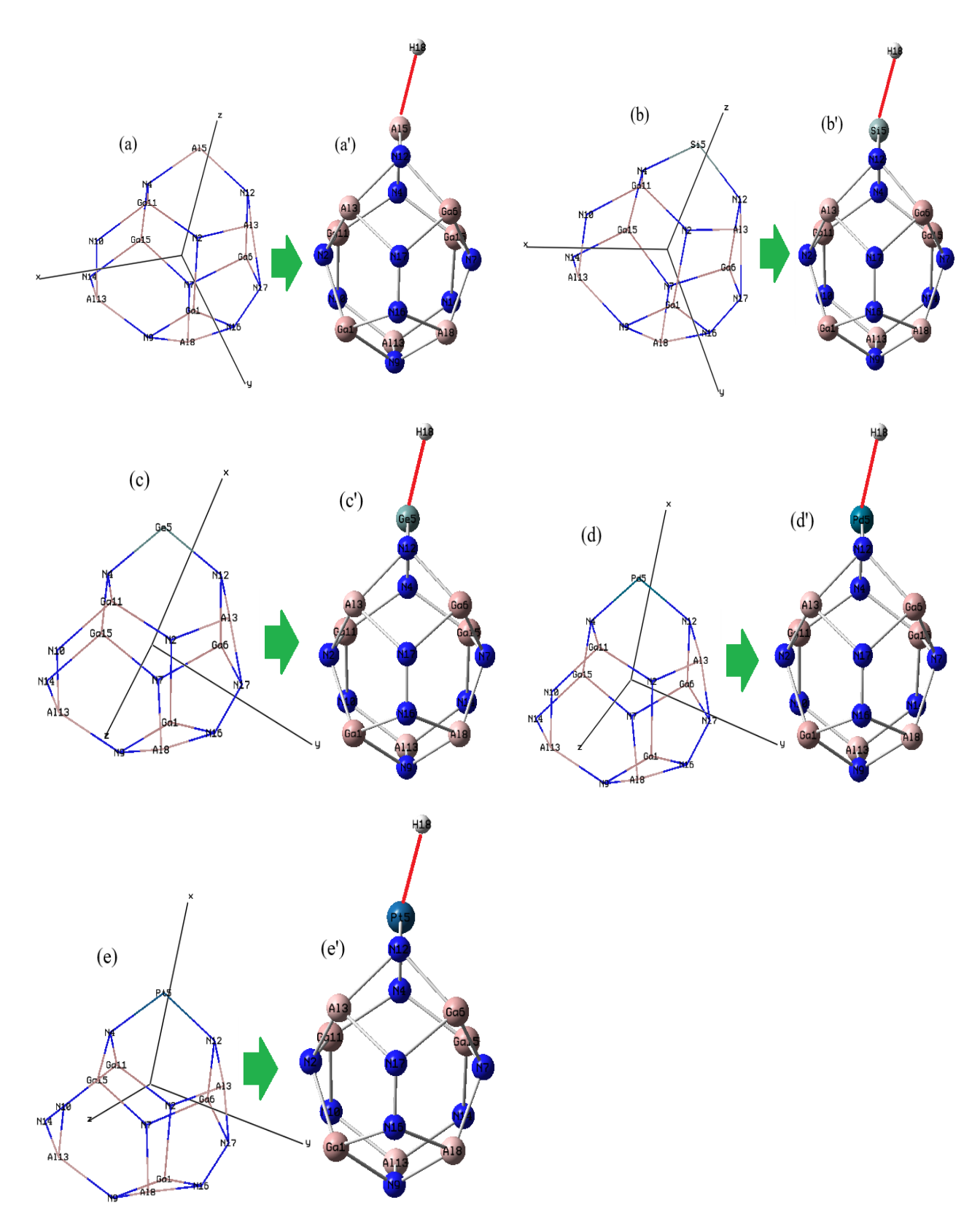


Figure 1. Characterization of (a) AlGaN, (b) AlGaSiN, (c) AlGaGeN, (d) AlGaPdN, and (e) AlGaPtN nanohybrids through a labeled ring in clockwise manner towards formation the hydrogenated nanoclusters of (a') H–AlGaN, (b') H–AlGaSiN, (c') H–AlGaGeN, (d') H–AlGaPdN, and (e') H–AlGaPtN.

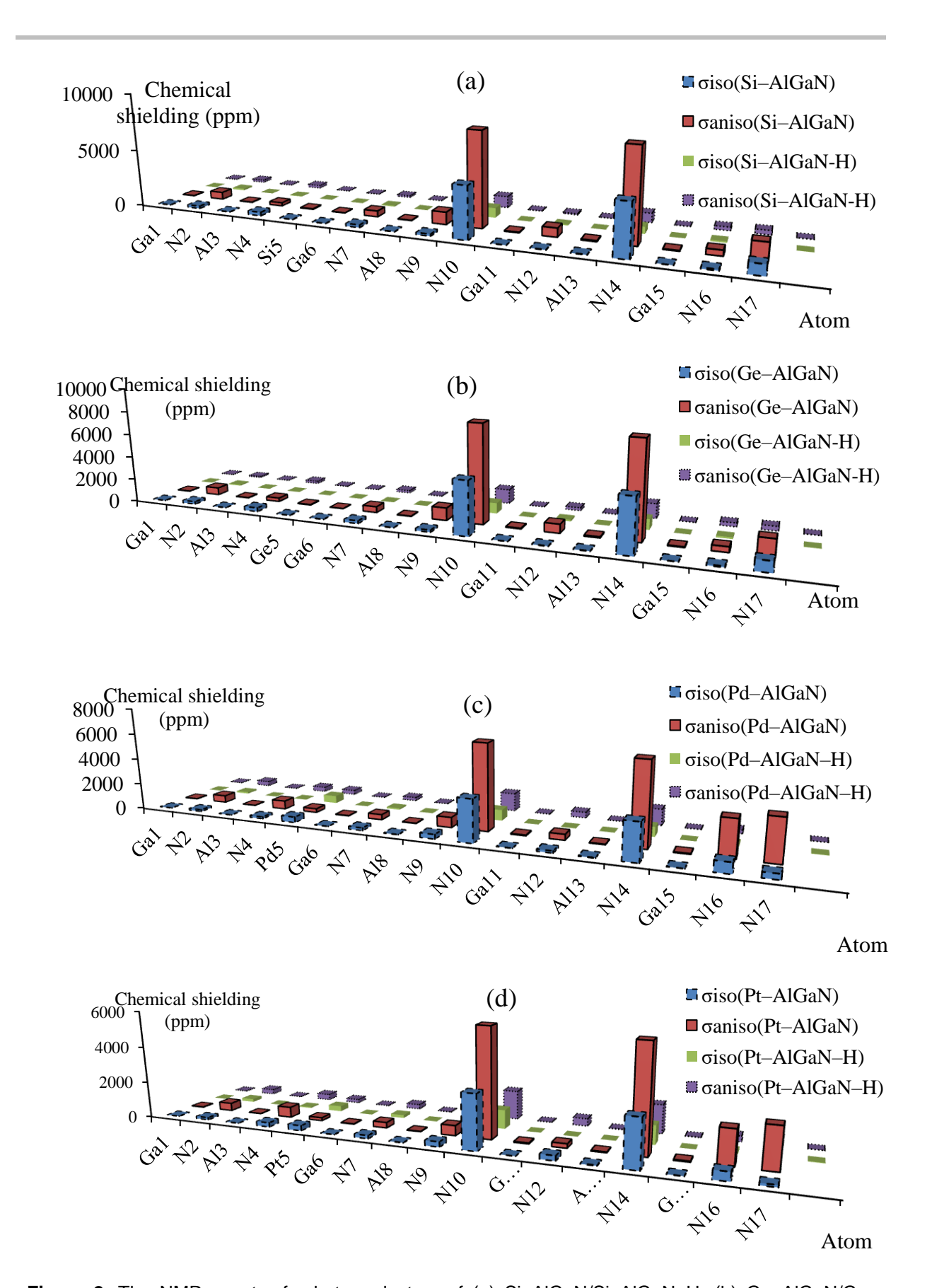


Figure 2. The NMR spectra for hetero-clusters of (a) Si–AlGaN/Si–AlGaN–H, (b) Ge–AlGaN/Ge–AlGaN–H, (c) Pd–AlGaN/Pd–AlGaN–H, (d) Pt–AlGaN/Pt–AlGaN–H.

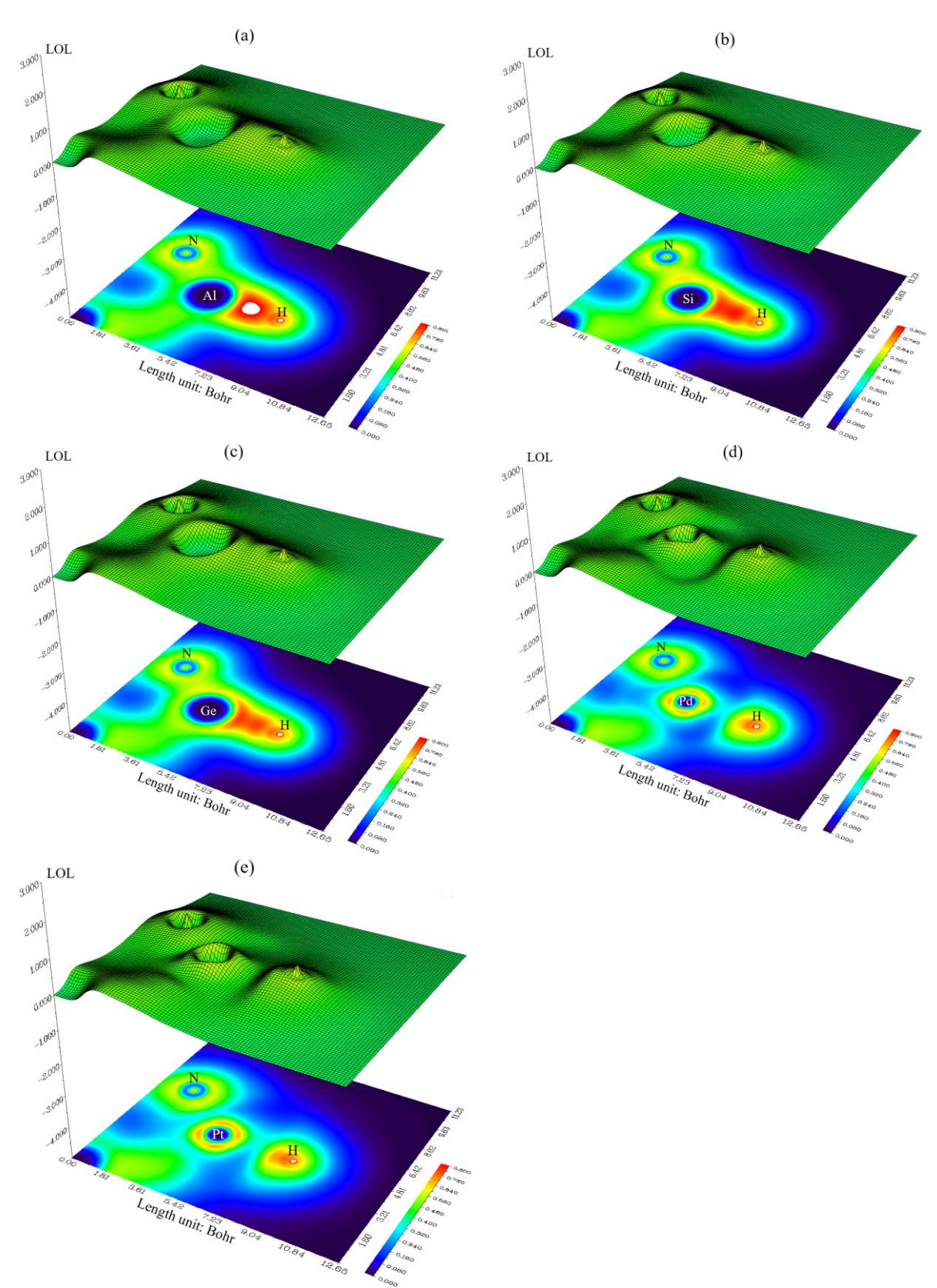


Figure 3. The shaded graphs of LOL for hetero-clusters include (a) H–AlGaN, (b) H–AlGaSiN, (c) H–AlGaGeN, (d) H–AlGaPdN, and (e) H–AlGaPtN.

The notable fragile signal intensity close to the parallel edge of the nanocluster sample might be owing to silicon or germanium binding induced non-spherical distribution of Si–AlGaN (Figure 2a) or Ge–AlGaN (Figure 2b) hetero-clusters. Figure 2 (c, d) exhibited the same tendency of shielding for palladium or platinum; however, a considerable deviation exists from doping atoms of palladium or platinum as electron acceptors on the surface of Pd–AlGaN or Pt–AlGaN hetero-clusters.

The observed increase in the chemical shift anisotropy spans for nanocages of Si-AlGaN/Si-AlGaN-H (Figure 2a) and Ge-AlGaN/Ge-AlGaN-H (Figure 2b) is near N (10), N (14), N (17). The yield of electromagnetic shifting can be directed by the mentioned active nitrogen atoms extracted from ternary hybrid hereto-clusters. It has shown that the intensity for energy storage can be enhanced in Pd-AlGaN (Figure 2c) and Pt-AlGaN (Figure 2d) through hydration and formation of Pd-AlGaN-H and Pt-AlGaN-H due to oscillating of chemical shielding in N(10), N(14), N(16), N(17) atoms. So, it can be observed that doped hetero-clusters of Si-AlGaN, Ge-AlGaN, Pd-AlGaN, Pt-AlGaN might ameliorate capability of AlGaN for energy storage.

Investigations of interstitial hydrogen diffusion play a key role in understanding fundamental properties of hydrogen storage materials since the activation energy required to jump from one interstitial site to other affects both the hydrogen sorption kinetics and the desorption temperature. Nuclear magnetic resonance is a very effective tool to study hydrogen diffusivity, jump frequency etc. but it cannot describe the microscopic hydrogen migration processes. From this perspective theoretical studies are very helpful and complement the experiment, however, the results depend on the quality of calculations.

Localized orbital locator (LOL) has similar expression compared to electron localization function (ELF) [30].

LOL(**r**) =
$$\frac{\tau(\mathbf{r})}{1+\tau(\mathbf{r})}$$
;

$$\tau(\mathbf{r}) = \frac{D_0(\mathbf{r})}{\frac{1}{2} \sum_i \eta_i |\nabla \varphi_i(\mathbf{r})|^2}$$
(1)

$$D_0(\mathbf{r}) = \frac{3}{10} (6\pi^2)^{2/3} [\rho_\alpha(\mathbf{r})^{5/3} + \rho_\beta(\mathbf{r})^{5/3}]$$

Multiwfn [31–33] also supports the approximate version of LOL defined by Tsirelson and Stash [34], namely the actual kinetic energy term in LOL is replaced by second-order gradient expansion like ELF which may demonstrate a broad span of bonding samples. This Tsirelson's version of LOL can be activated by

setting "ELFLOL_type" to 1. For special reason, if "ELFLOL_type" in settings.ini is changed from 0 to 2, another formalism will be used:

$$LOL(\mathbf{r}) = \frac{1}{1 + \left[1/\tau(\mathbf{r})\right]^2}$$
 (3)

If the parameter "ELFLOL_cut" in settings.ini is set to x, then LOL will be zero where LOL is less than x. The compounds of H-AlGaN, H-AlGaSiN, H-AlGaGeN, H-AlGaPdN, and H-AlGaPtN can be defined by LOL graphs owing to exploring their delocalization/localization characterizations of electrons and chemical bonds (Figure 3a-e).

The counter map of LOL for H-AIGaN has shown the electron delocalization due to labeling atoms of N(4), Al (5), H (18) (Figure 3a). Then, hydration of Si- and Ge-doped AlGaN indicates a larger isosurface map of electron delocalization due to labeling atoms of N(4), Si (5), H (18) of AlGaSiN -H (Figure 3b) and N(4), Ge (5), H (18) of H-AlGaGeN (Figure 3c). A vaster jointed area engaged by an isosurface map for Pd and Pt doping AlGaN towards formation of hetero-clusters AlGaPdN -H (Figure 3d) and H-AlGaPtN (Figure 3e) after hydrogen adsorption due to labeling atoms of N(4), Pd/Pt(5), H (18), respectively. A narrower connected area occupied by an isosurface map means that electron delocalization is relatively difficult. However, the large counter map of LOL for H-H-AlGaPdN. H-AlGaSiN, AlGaPtN. AlGaGeN can confirm that doping Pd, Pt, Si, Ge nanoparticles on the surface, increases the efficiency of ternary heterocluster of AlGaN for energy storage. Besides, the changes of charge density analysis have illustrated that AlGaN has shown the Bader charge of -1.272 coulomb, and after doping with silicon, germanium, palladium, platinum has indicated the Bader charge of -1.290, -1.285, -1.292, -1.309 coulomb for AlGaSiN, AlGaGeN, AlGaPtN, AlGaPdN, respectively, describes the tensity value of these heteroclusters for energy storage.

Moreover, intermolecular orbital overlap integral is important in discussions of intermolecular charge transfer which can calculate HOMO-HOMO and LUMO-LUMO overlap integrals between the hydrogen atom and hybrid hetero-clusters of AlGaN, AlGaSiN, AlGaGeN, AlGaPdN, AlGaPtN. The wavefunction level we used is CAM-B3LYP-D3/6-311+G(d, p) that correspond to HOMO and LUMO, respectively (Table1).

Hetero-clusters	E _{LUMO} (a.u.)	E _{HOMO} (a.u.)	$\Delta E = E_{LUMO} - E_{HOMO}$ (a.u.)	< S ² >
H–AlGaN	-0.1550	-0.1846	0.0296	1.7500
H-AlGaSiN	-0.1531	-0.1833	0.0302	2.0022
H–AlGaGeN	-0.1519	-0.1822	0.0303	2.6557
H-AlGaPdN	-0.1499	-0.1780	0.0281	2.6260
H-AlGaPtN	-0.1513	-0.1791	0.0278	2.6349

Table1. LUMO/HOMO, energy gap (ΔE) and overlap integral for H–AlGaN, H–AlGaSiN, H–AlGaGeN, H–AlGaPdN, H–AlGaPtN.

This approach effectively captures the characteristics of the ligand field within TMs. Consequently, it delivers precise HOMO–LUMO gap predictions comparable to those achieved by three-dimensional information-based models while also demonstrating strong performance in predicting the heterocluster electronic properties.

For unrestricted wavefunctions, orthonormalization condition does not hold in general between alpha and beta orbitals. This function computes the overlap matrix between alpha and beta orbitals:

$$S_{i,j}^{\alpha,\beta} = \int \varphi_i^{\alpha}(r)\varphi_j^{\beta}(r)dr$$
 (4)
The diagonal elements are useful for

The diagonal elements are useful for evaluating the matching degree of corresponding spin orbital pairs, evident deviation to 1 indicates that spin polarization is remarkable. Because the expectation of S^2 operator for single determinant (SD) wavefunction can be easily derived from the matrix, Multiwfn [31–33] outputs this quantity together:

$$\langle S^2 \rangle_{SD} = \langle$$

 $S^2 \rangle_{Exact} + N^{\beta} - \sum_{i}^{N^{\alpha}} \sum_{j}^{N^{\beta}} \left| S_{i,j}^{\alpha,\beta} \right|^2$ (5)

where $\langle S^2 \rangle_{Exact}$ is the exact value of square of total spin angular momentum:

$$\langle S^2 \rangle_{Exact} = \frac{N^{\alpha} - N^{\beta}}{2} \left(\frac{N^{\alpha} - N^{\beta}}{2} + 1 \right)$$
 (6)

A strategy for increasing the square of an overlap integral (< $S^2>$) of electron in AlGaN is proposed by doping of Si, Ge, Pd, or Pt (Table 1). Therefore, E_{LUMO} (a.u.), E_{LUMO} (a.u.) and the local bandgap energies ($\Delta E/a.u.$) and immobile charges induced by polarization discontinuity are simultaneously controlled throughout the structures, and optimized band

profiles are eventually achieved for H–AlGaN, H–AlGaSiN, H–AlGaGeN, H–AlGaPdN, H–AlGaPtN. <S²> has been ameliorated after doping the semiconductor atoms of silicon, germanium and noble transition metals of palladium, platinum on the ternary AlGaN alloy for that might increase electron charge transfer in superconductor devices.

3.2. Analysis of Nuclear Quadrupole Resonance spectra

The NQR frequencies have been measured for AlGaSiN, AlGaGeN, AlGaPdN, AlGaPtN towards estimating the hydrogenated nanoclusters of H–AlGaSiN, H–AlGaGeN, H–AlGaPdN, H–AlGaPtN. The NQR method is related to the multipole expansion in Cartesian coordinates as the equation (7) [35–38]:

$$V(r) = V(0) + \left[\left(\frac{\partial V}{\partial x_i} \right) \Big|_{0} . x_i \right] + \frac{1}{2} \left[\left(\frac{\partial^2 V}{\partial x_i x_j} \right) \Big|_{0} . x_i x_j \right] + \cdots$$

$$(7)$$

$$U = -\frac{1}{2} \int_{\mathcal{D}} d^3 r \rho_r \left[\left(\frac{\partial^2 V}{\partial x_i^2} \right) \Big|_{0} . x_i^2 \right] =$$

$$-\frac{1}{2} \int_{\mathcal{D}} d^3 r \rho_r \left[\left(\frac{\partial E_i}{\partial x_i} \right) \Big|_{0} . x_i^2 \right] =$$

$$-\frac{1}{2} \left(\frac{\partial E_i}{\partial x_i} \right) \Big|_{0} . \int_{\mathcal{D}} d^3 r \left[\rho(r) . x_i^2 \right]$$

$$(8)$$

The interaction nuclear of а with moment quadrupole the local inhomogeneous electric field removes the degeneracy of the nuclear ground state. The transition frequencies between the nuclear quadrupole energy levels, which are typically in the MHz frequency region, depend on the nuclear quadrupole moment and on the electric field gradient tensor at the nucleus. The "electric potential" through carrying over the electric charge was measured for AlGaSiN/H- AlGaSiN, AlGaGeN/H- AlGaGeN, AlGaPdN/H- AlGaPdN, AlGaPtN/H- AlGaPtN

complexes. Al, Ga, Si, Ge, Pd, Pt, N and the hydrogen atom absorbed on AlGaN, AlGaSiN, AlGaGeN, AlGaPdN, AlGaPtN have been calculated through the "Bader charge" and electronic potential properties (Tables 2&3). The elements of N2, N4, N7, N9, N10, N12,

N14 of AlGaN, AlGaSiN, AlGaGeN, AlGaPdN, AlGaPtN have exhibited the most efficiency for admitting the electron from "electron donor" of H18 adsorbed on AlGaN, AlGaSiN, AlGaGeN, AlGaPdN, AlGaPtN (Tables 2&3).

Table 2. Data of Bader charge (Q/Coulomb) and potential energy ($E_p/a.u.$) for AlGaSiN, H-AlGaSiN, AlGaGeN, H-AlGaGeN hetero-clusters.

AlGaSiN			H–AlGaSiN			AlGaGeN			H–AlGaGeN			
Atom	Q	E_p	Atom	Q	E_p	Atom	Q	E_p	Atom	Q	E_{p}	
Ga1	1.0145	-1.2293	Ga1	0.9919	-1.2418	Ga1	1.0106	-1.2310	Ga	0.9784	-1.2470	
N2	-1.1427	-18.3948	N2	-1.1462	-18.4011	N2	-1.1420	-18.3962	N2	-1.1475	-18.4047	
Al3	1.2522	-1.2023	Al3	1.2832	-1.2007	Al3	1.2476	-1.2043	A13	1.2976	-1.2024	
N4	-1.1045	-18.4112	N4	-1.0695	-18.3870	N4	-1.0930	-18.4185	N4	-1.0819	-18.3962	
Si5	0.7566	-1.8973	Si5	0.7501	-1.8495	Ge5	0.7604	-1.8300	Ge	0.6899	-1.8020	
Ga6	0.9752	-1.2344	Ga6	0.9583	-1.2420	Ga6	0.9708	-1.2364	Ga	0.9852	-1.2364	
N7	-1.1268	-18.3991	N7	-1.1213	-18.4082	N7	-1.1269	-18.4005	N7	-1.1483	-18.4017	
Al8	1.2902	-1.1990	Al8	1.2802	-1.2115	Al8	1.2854	-1.2007	Al8	1.2668	-1.2103	
N9	-1.1861	-18.4051	N9	-1.1838	-18.4157	N9	-1.1864	-18.4065	N9	-1.2073	-18.4157	
N10	-0.7902	-18.4041	N10	-0.7725	-18.4174	N10	-0.7894	-18.4050	N1	-0.7707	-18.4142	
Ga11	1.0153	-1.2386	Ga11	1.0639	-1.2317	Ga11	1.0092	-1.2406	Ga	1.0702	-1.2337	
N12	-1.1390	-18.3958	N12	-1.1318	-18.3903	N12	-1.1251	-18.4022	N1	-1.1185	-18.3988	
Al13	1.1938	-1.2237	Al13	1.2028	-1.2280	Al13	1.1914	-1.2251	Al1	1.2308	-1.2200	
N14	-0.7775	-18.4005	N14	-0.8328	-18.4281	N14	-0.7773	-18.4014	N1	-0.7833	-18.4186	
Ga15	1.0280	-1.2408	Ga15	1.0092	-1.2441	Ga15	1.0223	-1.2428	Ga	1.0407	-1.2385	
N16	-0.6448	-18.3454	N16	-0.6320	-18.3565	N16	-0.6448	-18.3467	N1	-0.6289	-18.3568	
N17	-0.6142	-18.3417	N17	-0.6327	-18.3549	N17	-0.6129	-18.3432	N1	-0.6330	-18.3548	
			H18	-0.0174	-1.0120				H1	-0.0401	-1.0384	

Table 3. Data of Bader charge (Q/Coulomb) and potential energy (E_p /a.u.) for AlGaPdN, H–AlGaPdN, AlGaPtN, and H–AlGaPtN hetero-clusters.

AlGaPdN			H–AlGaPdN			AlGaPtN			H–AlGaPtN		
Atom	Q	E _p	Atom	Q	E _p	Atom	Q	E _p	Atom	Q	E _p
Ga1	1.0197	-1.2296	Ga1	1.0144	-1.2281	Ga1	1.0296	-1.2264	Ga1	1.0120	-1.2306
N2	-1.1542	-18.3993	N2	-1.1640	-18.3900	N2	-1.1551	-18.3956	N2	-1.1543	-18.3964
Al3	1.2464	-1.2103	A13	1.2954	-1.1935	A13	1.2607	-1.2042	Al3	1.2596	-1.2012
N4	-0.8860	-18.3944	N4	-0.9111	-18.3861	N4	-0.9550	-18.3833	N4	-1.0208	-18.3769
Pd5	0.3351	-16.3098	Pd5	0.1988	-16.2830	Pt5	0.4083	-14.8314	Pt5	0.2914	-14.8045
Ga6	0.9649	-1.2440	Ga6	0.9996	-1.2295	Ga6	0.9764	-1.2381	Ga6	0.9953	-1.2327
N7	-1.1344	-18.4034	N7	-1.1330	-18.3955	N7	-1.1356	-18.3993	N7	-1.1495	-18.396
Al8	1.2922	-1.1996	Al8	1.3138	-1.1960	Al8	1.3086	-1.1963	Al8	1.2820	-1.1996
N9	-1.1921	-18.4049	N9	-1.1890	-18.403	N9	-1.1911	-18.4030	N9	-1.2098	-18.4017
N10	-0.8065	-18.4116	N10	-0.7750	-18.4130	N10	-0.8109	-18.4112	N10	-0.7700	-18.4067
Gal1	1.0388	-1.2424	Ga11	1.0760	-1.2289	Ga11	1.0590	-1.2374	Ga11	1.0862	-1.2273
N12	-0.9359	-18.3900	N12	-0.9211	-18.3801	N12	-1.0113	-18.3763	N12	-0.9789	-18.3696
Al13	1.2001	-1.2232	Al13	1.2236	-1.2161	Al13	1.2068	-1.2217	Al13	1.2564	-1.2058
N14	-0.7799	-18.4018	N14	-0.8321	-18.4186	N14	-0.7850	-18.401	N14	-0.7735	-18.4056
Ga15	1.0385	-1.2439	Ga15	1.0614	-1.2349	Ga15	1.0583	-1.2388	Ga15	1.0974	-1.2264
N16	-0.6380	-18.3426	N16	-0.6337	-18.3452	N16	-0.6441	-18.3438	N16	-0.6373	-18.3475
N17	-0.6087	-18.3426	N17	-0.6319	-18.3448	N17	-0.6196	-18.3423	N17	-0.6264	-18.3476
			H18	0.0080	-1.0864				H18	0.0402	-1.0880

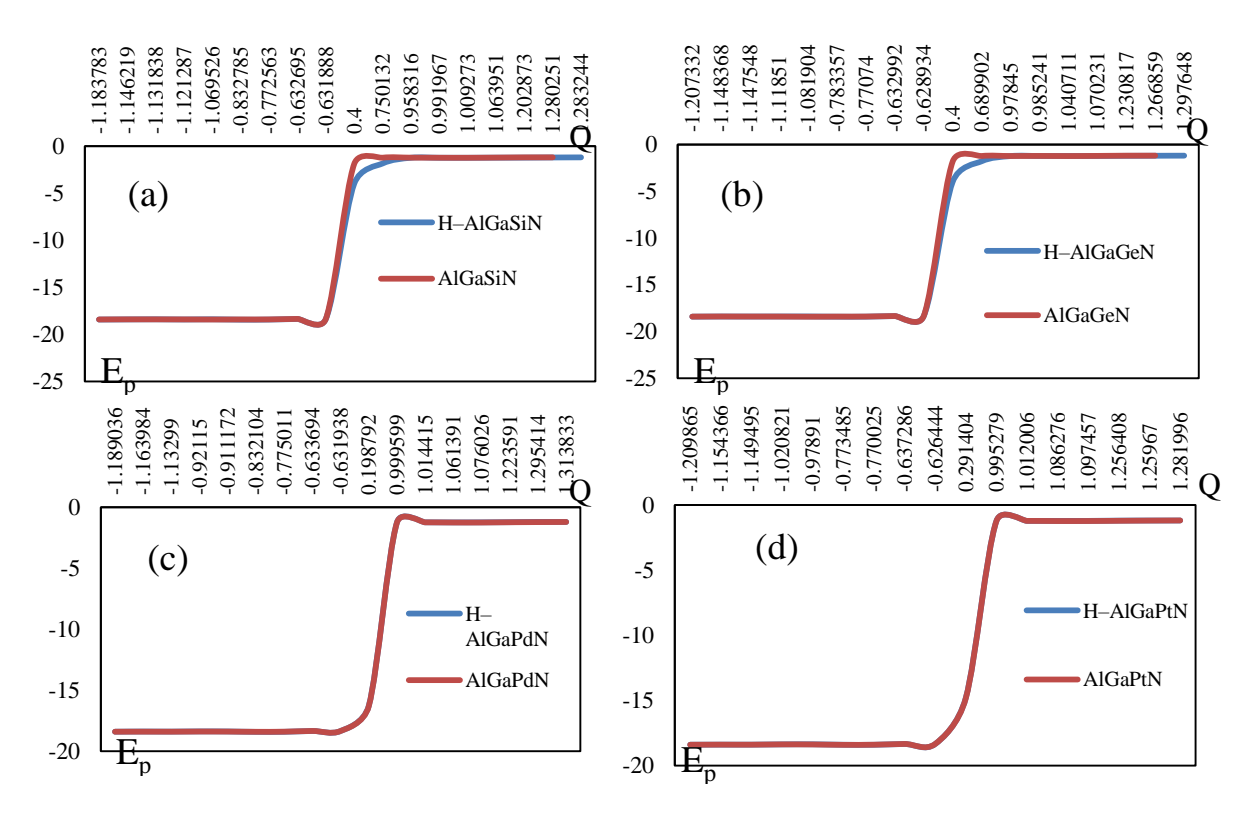
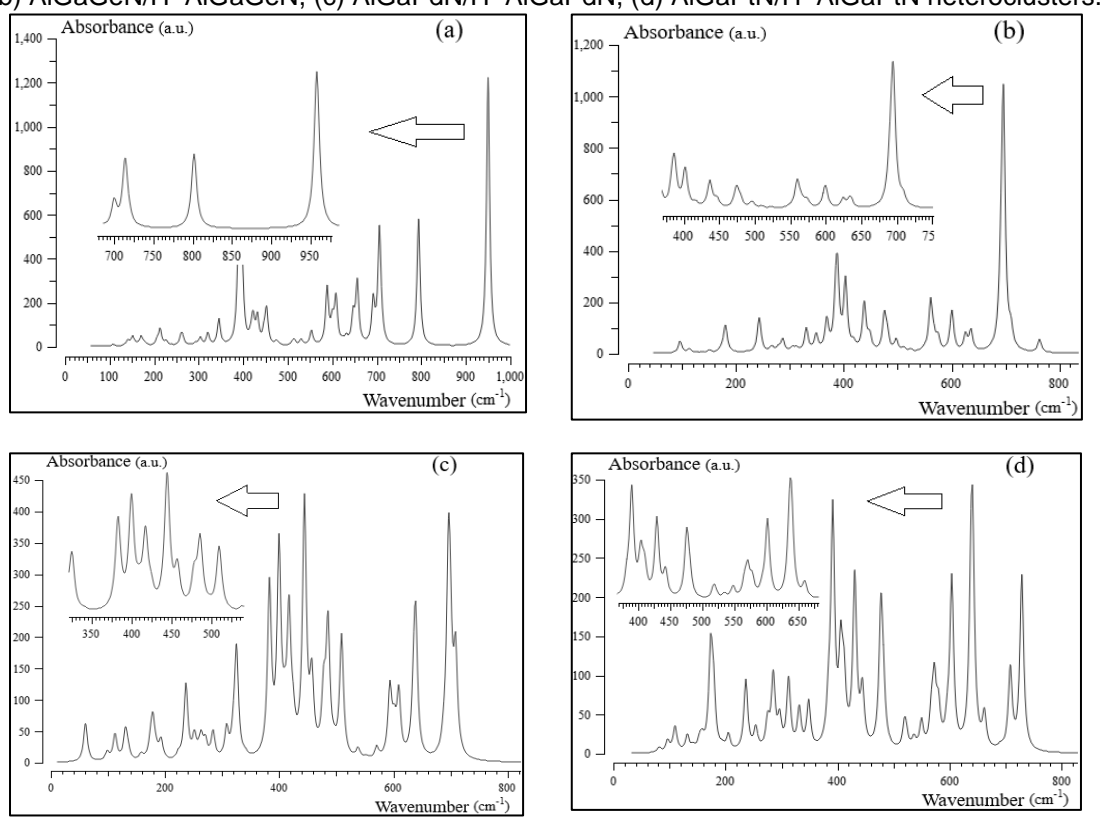


Figure 4. The graph of potential energy (E_p) versus atomic charge (Q) for (a) AlGaSiN/H–AlGaSiN, (b) AlGaGeN/H–AlGaGeN, (c) AlGaPdN/H–AlGaPdN, (d) AlGaPtN/H–AlGaPtN heteroclusters.



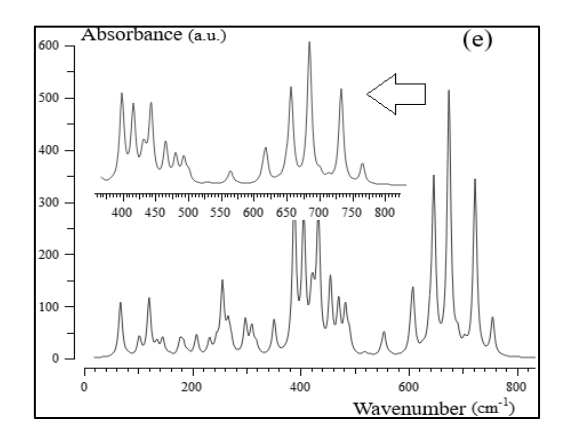


Figure 5. The wavenumber (cm⁻¹) changes through the IR spectra for hetero-clusters of (a) H–AlGaN, (b) H–AlGaSiN, (c) H–AlGaGeN, (d) H–AlGaPdN, and (e) H–AlGaPtN.

In Figure 4 (a–d), it has been drawn the electric potential versus Bader charge for Al, Ga, Si, Ge, Pd, Pt, N and the hydrogen atom absorbed on AlGaSiN, AlGaGeN, AlGaPdN, AlGaPtN.

It was observed the similar behavior of hydrogen adsorption by AlGaSiN, AlGaGeN (Figure4a,b) through high sensitivity based on relation coefficient about $R^2 = 0.997$. Moreover, AlGaPdN, AlGaPtN have indicated the similar behavior for hydrogen adsorption with relation coefficient about $R^2 = 0.998$ (Figure 4c,d).

The fluctuated peaks for electric potential have been shown around hydrogen adsorption on the AlGaSiN, AlGaGeN, AlGaPdN, AlGaPtN which demonstrates the electron accepting of hydrogen by Si, Ge, Pd and Pt atoms (Figure 4a–d).

3.3. Insight of infrared spectroscopy & thermochemistry

The infrared spectroscopy (IR) has been performed for ternary nanocage of AlGaN (Figure 5a) and hybrid alloys of AlGaSiN (Figure 5b), AlGaGeN (Figure 5c), AlGaPdN (Figure 5d), AlGaPtN (Figure 5e) through hydrogen adsorption.

CONCLUSION

In summary, hydrogen grabbing on the heteroclusters of AlGaN, AlGaSiN, AlGaGeN, AlGaPdN, and AlGaPtN for energy storage were investigated by first-principles calculations. We have provided a ternary semiconductor of aluminum gallium nitride which is doped with silicon, germanium, palladium or platinum. The geometrical parameters of doping atoms on the surface of AlGaN through the absorption status and current charge density of the energy storage

was studied. Moreover, the effect of a relative chemical shift between AlGaN and doped heteroclusters also investigated. was Thermodynamic parameters have constructed a detailed molecular model for atom-atom interactions and a distribution of point charges which can be utilized to reproduce the polarity of the solid material and the adsorbing molecules. Energy storage with heteroclusters described that the frame overcoming cluster is related to AlGaPdN or AlGaPtN in the high amounts of frequency. This property makes AlGaPdN or AlGaPtN potentially advantageous for certain highfrequency applications for energy storage due to hydrogen adsorption by formation of H-AlGaN, H-AlGaSiN, H-AlGaGeN, H-AlGaPdN or H-AlGaPtN. The advantages of platinum or palladium over aluminum gallium nitride include its higher electron and hole mobility, allowing platinum or palladium doping devices to operate at higher frequencies than silicon or germanium doping devices. Thus, it should be explored its unique properties, such as its ability to increase energy storage in devices.

Acknowledgements

The author is grateful to Kastamonu University for completing this paper and its research.

REFERENCES

- [1] M. L. Nakarmi, N. Nepal, J. Y. Lin and H. X. Jiang, Appl. Phys. Lett., 2009, 94, 091903.
- [2] K. B. Nam, J. Li, M. L. Nakarmi, J. Y. Lin and H. X. Jiang, Appl. Phys. Lett., 2002, 81, 1038–1040.
- [3] J. P. Zhang, X. Hu, Y. Bilenko, J. Deng, A. Lunev, M. S. Shur, R. Gaska, M. Shatalov, J. W. Yang and M. A. Khan, Appl. Phys. Lett., 2004, 85, 5532–5534.

- [4] Mollaamin, F. Monajjemi, M. Unraveling Hetero-Clusters of Indium Gallium Nitride and Its Alloys for Solar Cells Development: Structural and Characterization Study of Nitride-Based Semiconductors Using DFT Framework. Russ. J. Phys. Chem. B 19, 480–500 (2025).
- [5] T. Kinoshita, T. Obata, H. Yanagi and S.-I. Inoue, Appl. Phys. Lett., 2013, 102, 012105.
- [6] Z. Jun, T. Wu, W. Feng, Y. Weiyi, X. Hui, D. Jiangnan, F. Yanyan, W. Zhihao and C. Changqing, IEEE Photonics J., 2013, 5, 1600310.
- [7] Mollaamin, F. Monajjemi, M. Doping Effects in Ternary Aluminum Gallium Nitride Hetero-Cluster Towards High-Electron-Mobility Transistors for Hydrogen Sensing: A Density Functional Theory Study and Energy-Saving. Russ. J. Phys. Chem. B 19, 236–254 (2025). https://doi.org/10.1134/S199079312470 168
- [8] Mollaamin, F. Monajjemi, M. Structural, Electromagnetic and Thermodynamic Analysis of Ion Pollutants Adsorption in Water by Gallium Nitride Nanomaterial: a Green Chemistry Application. Russ. J. Phys. Chem. B 18, 533–548 (2024). https://doi.org/10.1134/S199079312402 012X
- [9] Sipan Yang, Jianchang Yan, Miao He, Kunhua Wen, Yanan Guo, Junxi Wang, Deping Xiong & Huan Yin, Influence of Silicon-Doping in n-AlGaN Layer on the Optical and Electrical Performance of Deep Ultraviolet Light-Emitting Diodes. Russ. J. Phys. Chem. 93, 2817– 2823 (2019). https://doi.org/10.1134/S003602441913 034X
- [10] R. Blasco, A. Ajay, E. Robin, C. Bougerol, K. Lorentz, L.C. Alves, I. Mouton, L. Amichi, A. Grenier and E.Monroy, J. Phys. D: Appl. Phys. 52, 125101, 2019. DOI: 10.1088/1361-6463/aafec2
- [11] Danhao WangXin LiuShi FangChen HuangYang KangHuabin YuZhongling LiuHaochen ZhangRan LonaYuiie XiongYangjian LinYang YueBinghui GeTien Khee NgBoon S. OoiZetian MiJr-Hau HeHaiding Sun, Pt/AlGaN Nanoarchitecture: Toward Responsivity, Self-Powered Ultraviolet-Sensitive Photodetection. Nano Lett. 2021, 120-129. 21, 1,

- https://doi.org/10.1021/acs.nanolett.0c03
- [12] Mollaamin, F. Anchoring of 2D layered materials of Ge₅Si₅O₂₀ for (Li/Na/K)-(Rb/Cs) batteries towards Eco-friendly energy storage. *BMC Chemistry* 19, 233 (2025).
- [13] Perdew, J.P.; Burke, K.; Ernzerhof, M. Generalized gradient approximation made simple. Phys. Rev. Lett. 1996, 77, 3865.
- [14] Mollaamin, F. Competitive Intracellular Hydrogen-Nanocarrier Among Silicon Aluminum, Carbon, or Implantation: a Novel Technology of Eco-Friendly Energy Storage using Research Density **Functional** Theory. Russ. J. Phys. Chem. B 18, 805-820 (2024).https://doi.org/10.1134/S199079312470 0131
- [15] Arrigoni, M.; Madsen, G.K.H. Comparing the performance of LDA and GGA functionals in predicting the T lattice thermal conductivity of III-V semiconductor materials in the zincblende structure: The cases of AlAs and BAs. Comput. Mater. Sci. 2019, 156, 354–360.
- [16] Hohenberg, P.; Kohn, W. Inhomogeneous Electron Gas. Phys. Rev. B, 1964, 136, B864-B871.
- [17] Kohn, W.; Sham, L. J. Self-Consistent Equations Including Exchange and Correlation Effects.Phys. Rev., 1965, 140, A1133- A1138.
- [18] Becke AD (1993) Density-functional thermochemistry. III. The role of exact exchange. J Chem Phys 98:5648–5652.
- [19] Lee C, Yang W, Parr RG (1988)
 Development of the Colle–Salvetti
 correlation-energy formula into a
 functional of the electron density. Phys
 Rev B 37:785–789.
- [20] K. Kim; K. D. Jordan (1994). "Comparison of Density Functional and MP2 Calculations on the Water Monomer and Dimer". J. Phys. Chem. 98 (40): 10089–10094. doi:10.1021/j100091a024.
- [21] Mollaamin, F. Investigating the Treatment of Transition Metals for Ameliorating the Ability of Boron Nitride for Gas Sensing & Removing: A Molecular Characterization by DFT Framework. Prot Met Phys Chem Surf 60, 1050–1063 (2024).
- [22] Mollaamin, F. Alkali Metals Doped on Tin-Silicon and Germanium-Silicon

- Oxides for Energy Storage in Hybrid Biofuel Cells: A First-Principles Study. Russ. J. Phys. Chem. B 19, 722–736 (2025). https://doi.org/10.1134/S199079312570 0393
- [23] Mollaamin, F. Monajjemi, M. Adsorption ability of Ga_5N_{10} nanomaterial for removing metal ions contamination from drinking water by DFT, Int J Quantum Chem, 2024, 124, e27348. https://doi.org/10.1002/qua.27348.
- [24] Mollaamin, F. Monajjemi, M. Molecular modelling framework of metal-organic clusters for conserving surfaces: Langmuir sorption through the TD-DFT/ONIOM approach. Molecular 2023: 49(4): 365-376. Simulation. https://doi.org/10.1080/08927022.2022.2 159996.
- [25] Mollaamin, F. Monajjemi, M. Divulge of Hydrogen Energy Storage by Manganese Doped Nitrogen Nanocomposites of Aluminum, Gallium or Indium Nitrides: A First-Principles Study. Russ. J. Phys. Chem. B 19, 319– 335 (2025). https://doi.org/10.1134/S199079312570 006X
- [26] Frisch, M. J.; Trucks, G. W.; Schlegel, H. B.; Scuseria, G. E.; Robb, M. A.; Cheeseman, J. R.; Scalmani, G.; Barone, V.; Petersson, G. A.; Nakatsuji, H.; Li, X.; Caricato, M.; Marenich, A. V.; Bloino, J.; Janesko, B. G.; Gomperts, R.; Mennucci, B.; Hratchian, H. P.; Ortiz, J. V.; Izmaylov, A. F.; Sonnenberg, J. L.; Williams-Young, D.; Ding, F.; Lipparini, F.; Egidi, F.; Goings, J.; Peng, B.; Petrone, A.; Henderson, T.; Ranasinghe, D.; Zakrzewski, V. G.; Gao, J.; Rega, N.; Zheng, G.; Liang, W.; Hada, M.; Ehara, M.; Toyota, K.; Fukuda, R.; Hasegawa, J.; Ishida, M.; Nakajima, T.; Honda, Y.; Kitao, O.; Nakai, H.; Vreven, T.; Throssell, K.; Montgomery, J. A., Jr.; Peralta, J. E.; Ogliaro, F.; Bearpark, M. J.; Heyd, J. J.; Brothers, E. N.; Kudin, K. N.; Staroverov, V. N.; Keith, T. A.; Kobayashi, R.; Normand. J.: Rendell, A. Raghavachari, K.; Burant, J. C.; Iyengar, S. S.; Tomasi, J.; Cossi, M.; Millam, J. M.; Klene, M.; Adamo, C.; Cammi, R.; Ochterski, J. W.; Martin, R. L.; Morokuma, K.; Farkas, O.; Foresman, J. B.; Fox, D. J. Gaussian, Wallingford CT, 2016. 27.GaussView. Version 6.06.16, Dennington, Roy; Keith, Todd A.; Millam,

- John M. Semichem Inc., Shawnee Mission, KS, 2016.
- [27] Stefan Grimme, Jens Antony, Stephan Ehrlich, Helge Krieg, A consistent and accurate ab initio parametrization of density functional dispersion correction (DFT-D) for the 94 elements H-Pu. J Chem Phys. 2010, 132(15):154104. doi: 10.1063/1.3382344.
- [28] Sohail, U.; Ullah, F.; Binti Zainal Arfan, N.H.; Abdul Hamid, M.H.S.; Mahmood, T.; Sheikh, N.S.; Ayub, K. Transition Metal Sensing with Nitrogenated Holey Graphene: A First-Principles Investigation. Molecules 2023, 28, 4060. https://doi.org/10.3390/molecules
- [29] H.L Schmider, A.D Becke, Chemical content of the kinetic energy density. Journal of Molecular Structure: THEOCHEM. 527(1–3), 51-61 (2000). https://doi.org/10.1016/S0166-1280(00)00477-2
- [30] T. Lu & F. Chen, Multiwfn: a multifunctional wavefunction analyzer. J. Comput. Chem. 33, 580–592 (2012). doi:10.1002/jcc.22885
- T. Lu, A comprehensive electron wavefunction analysis toolbox for chemists, Multiwfn. J. Chem. Phys. 161, 082503 (2024). doi:10.1063/5.0216272
- [31] T. Lu & F. Chen, Meaning and Functional Form of the Electron Localization Function. Acta Phys. Chim. Sin. 27, 2786–2792(2011). doi:org/10.3866/PKU.WHXB20112786
- [32] V. Tsirelson and A. Stash, Analyzing experimental electron density with the localized-orbital locator. Acta Cryst. B58, 780-785 (2002). https://doi.org/10.1107/S010876810201 2338
- [33] Trontelj, Z.; Pirnat, J.; Jazbinšek, V.; Lužnik, J.; Srčič, S.; Lavrič, Z.; Beguš, S.; Apih, T.; Žagar, V.; Seliger, J. Nuclear Quadrupole Resonance (NQR)—A Useful Spectroscopic Tool in Pharmacy for the Study of Polymorphism. Crystals 2020, 10, 450. https://doi.org/10.3390/cryst10060450.
- [34] Sciotto, R.; Ruiz Alvarado, I.A.; Schmidt, W.G. Substrate Doping and Defect Influence on P-Rich InP(001):H Surface Properties. Surfaces 2024, 7, 79-87. https://doi.org/10.3390/surfaces7010006
- [35] Luo,J., Wang,C., Wang ,Z., Guo,Q., Yang,J., Rui Zhou, R., Matano,K., Oguchi,T., Ren, Z., NMR and NQR studies on transition-metal arsenide

superconductors LaRu2As2, KCa2Fe4As4F2, and A2Cr3As3*, Chinese Physm, 2020, B 29, 067402. https://doi.org/10.1088/1674-1056/ab892d.

[36] Young, Hugh A.; Freedman, Roger D. (2012). Sears and Zemansky's University Physics with Modern Physics (13th ed.). Boston: Addison-Wesley. p. 754.